

PARAMETER DETERMINATION FOR MODELLING THE ASTM A471 STEEL BEHAVIOUR IN AN ELASTO-PLASTIC CONTINUUM APPROACH

Fulvio E. G. Chimisso

Depto. de Materiais e Construção

FURG – Fundação Universidade de Rio Grande – RS, Brasil

Supported by CNPq fellowship

Gianni Caligiana

Dipartimento di Ingegneria delle Costruzioni Meccaniche, Aeronautiche e di Metallurgia

DIEM - Facoltà di Ingegneria Università di Bologna, Bologna, Italia

***Abstract.** The present work is concerned with the determination of material parameters to model the inelastic behaviour of an ASTM A 471 steel (24CrNiMoV14-6, vacuum-treated alloy steel forgings) very often utilised for turbine generator shafts, turbine rotor disks and wheels. Turboalternator shafts suffer very heavy local strain during transients and accidental emergencies (short circuits, out of phase synchronisation, etc.). The experimental work has been performed by strain controlled, completely reversed push-pull low cycle fatigue tests, at room temperature, to determine the stable hysteresis loops and the cyclic curve. The tests have been performed with a servo-hydraulic INSTRON testing machine on ASTM standard specimens. The aims of the study are the characterisation of hardening parameters for an elasto-plastic continuum model, taking into account the use of continuum damage mechanics models into design and structural integrity assessment of mechanical components. Good correlation has been found between the curves modelled by the kinematic hardening parameters and those obtained by experimental fatigue tests.*

***Key words:** continuum mechanics, elasto-plastic behaviour, cyclic hardening, strain control, hysteresis loop and kinematic hardening.*

1. INTRODUCTION

The use of continuum mechanics theoretical models into design and structural integrity assessment of mechanical components, sometimes is restricted by the difficulties to find references about material constants obtained by experimental data. Identify the parameters to find the stable hysteresis loop in an elasto-plastic steel behaviour, is an important step concerning low cycle fatigue life studies.

The present work is concerned with the determination of material parameters, that appear in internal variables elasto-plastic theories, used to model the inelastic behaviour of an ASTM A 471 (vacuum-treated alloy steel forgings) very often utilised for turbine generator shafts, turbine rotor disks and wheels. Low cycle fatigue is significant in the study of turboalternator shafts behaviour because, at stress raisers (fillets, change of section, etc.), they suffer very heavy local strain during transients and accidental emergencies like as short circuits, out of

phase synchronisation, etc., even though the nominal applied stress remains well inside the elastic range. This situation, common to many mechanical components also in the automotive industries, is generally treated as a strain controlled problem, owing to the presence of a wide elastic zone surrounding the plastic zone, where stresses are higher than yield strength owing to the local stress raiser.

The experimental data are obtained by strain controlled low cycle fatigue push-pull tests to determine the stable hysteresis loops and the associated cyclic curve. The analysis of the experimental stress-strain hysteresis loops, are used to determine the stress-plastic strain hysteresis curves and the parameters associated to a non-linear kinematic hardening rule, to find the stable hysteresis loop model. A method to determine those parameters and their evolution related to the total strain is showed.

A continuum elasto-plastic model with internal variables is used to model the hysteresis stable loops and the theoretical results are compared with the experimental results to check the model behaviour. Theoretical and experimental results are showed in stress-strain, stress-plastic strain and kinematic hardening-plastic strain graphics.

The interpolation of the experimental values of kinematic parameters versus total strain and of the stress-strain values to determine the cyclic curves has been performed by utilising non linear regression tools of the MATHEMATICA package. The mean values of Young modulus and the elastic limit have been determined, according to normal distribution, by using the same package.

2. MATERIAL

The experimental data considered in this paper have been derived from a broad study undertaken with the aim of extending knowledge about the fatigue behaviour of turboalternator shafts. In this study the material tested is a A471 (28 NiCrMoV 14-6) rotor steel supplied by several factories involved in the production of electrical power plant components, ASTM (1994). This material, as all NiCrMoV steels, retains high mechanical characteristics in the whole extension of large forgings, has a high elongation, shows a 100% ductile fracture at room temperature and it is insensitive to embrittlement at working temperatures. This steel was vacuum treated during pouring of the ingot, in order to limit the content of hydrogen and other gases not desired (oxygen, nitrogen, etc.).

The chemical composition and the typical heat treatments for A 471 are reported in Table 1. Mechanical properties are listed in Table 2.

Table 1 – Chemical composition and typical heat treatments of A 471 rotor steel

Chemical Composition (%)										
C	Si	Mn	P	S	Cr	Mo	Ni	V	Al	Cu
0.28	0.07	0.23	0.008	0.004	1.63	0.42	3.59	0.09	0.009	0.06
Heat Treatment										
Tempered			940°C x 28 hrs.;			870°C x 28 hrs.;		630°C x 28 hrs.		
Quality Tempered			845°C x 19 hrs.;			630°C x 25 hrs.;				
Stress-relieving			570°C x 21 hrs.			furnace cooled		(17.2 °C/hrs.)		
			200°C			air cooled				

Table 2 – Mechanical properties of A471 rotor steel

Mechanical Properties					
0.02 Yield Strength (MPa)	Tensile Strength (MPa)	Elongation (%)	Reduction of Area (%)	KV (J)	FATT (°C)
520-655	585-725	20	70	136-193	-12/-14

3. EXPERIMENTAL PROCEDURES

Several tests have been performed to derive the basic data, Caligiana (1987), for the characterisation of the steel in push-pull low cycle and high cycle fatigue, in low cycle reversed torsion and combined bending and torsion. Experimental data utilised in the paper are obtained by push-pull strain controlled low cycle fatigue tests to determine the stable hysteresis loops and the cyclic curve.

Tests have been performed with an INSTRON servo-hydraulic testing machine, series 8000, on ASTM standard 12 mm diameter specimen. A triangular strain waveform at a constant total strain rate (1%/s) was applied and a clip-gage was used for measuring the total strain at room temperature. The specimens have been fixed to the testing apparatus through an accurately sized flanged joint (button-head fixture, Curioni, 1992), instead of the commonly utilised threads, with the aim of reducing clearances and possible bending in the loading train.

A set of specimens (E1 to E6) has been cycled with standard strain-controlled low cycle fatigue test, with strain amplitudes ranging between 0.46% and 1.27%. Here, due to the limited space, only the development of hysteresis behaviour for specimen E5 is shown in Figure 1, where the continuous softening phenomenon can be observed.

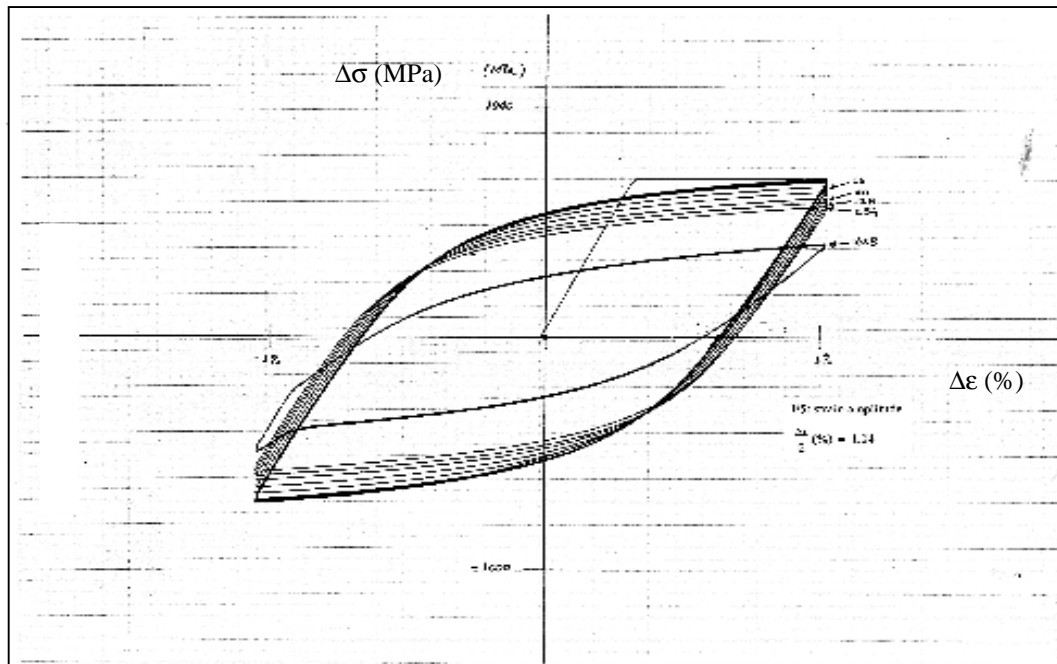


Fig.1 Strain-controlled low cycle fatigue test, specimen E5: $\Delta\epsilon/2 = 1.04\%$

Preliminary tests have shown a strong influence of bending on experimental results, also in the low cycle fatigue range. So, to prevent that undesirable effect, all the specimens utilised to derive the evolution of the hysteresis curve and of the basic fatigue data have been instrumented with strain gages. Before each test, the linearity and angularity of the loading train have been adjusted by means of suitable taper rings in series with the upper grip of the hydraulic machine. Actual bending is checked and measured through the strain gage readings of the instrumented specimens during loading ramps in the elastic field, preliminary to each test. During tests, bending has been continuously monitored and recorded until gage failure, to assure low bending during dynamic tests too. A bending strain lower than 7.5% of the total strain amplitude applied during the corresponding test is assured.

The companion specimen test (CST) where several specimens, each with a different strain amplitude, are cycled to failure between constant strain limits, is used to determine the experimental cyclic curve. Usually the cyclic curve is obtained by the tips connection of the hysteresis loops at saturation (when it is found) or at the half-life of test specimens.

Considering the little sample, a Student distribution are used to certify that a normal distribution of the Young modulus and of the elastic limit obtained in the experimental tests are a reasonable representation of those parameters. Consequently, mean values $E=186.5$ GPa and stable cycle elastic limit (at $\epsilon = 0.02\%$) $S_y = 545$ MPa, are used.

4. THE ELASTO-PLASTIC CONTINUUM MODEL

The set of elasto-plastic constitutive equations with internal variables used in this work describes the mechanical behaviour of metallic materials submitted to non-monotonic loading. We use the concept of the free energy in the constitutive theory with a strong thermodynamic basis, Lemaitre (1990). The free energy is defined as a differentiable function of the state variables: $\psi = \psi(\epsilon - \epsilon^p, \beta)$.

ϵ^p is the plastic strain and β is a generic representation of the other internal variables. The elastic dominion was defined by the existence of a plastic potential F such that

$$F(\sigma, B^\beta, \epsilon^p, \beta) < 0 \Rightarrow \dot{\epsilon}^p = 0 \text{ e } \dot{\beta} = 0 ; B^\beta = \frac{\partial \psi}{\partial \beta}$$

The elasto-plastic model proposed by Marquis (1978) and generalised by Costa Mattos (1989) is used in a unidimensional approach. A non-linear cinematic hardening rule proposed by Armstrong and Frederick (1966) is used to show the couple between plastic strain and kinematic hardening; a set of constitutive elasto-plastic model equations, with combined isotropic and kinematic hardening can be written as follows for a material obeying the von Mises criterion:

$$\sigma = \frac{\partial \psi}{\partial \epsilon} = E(\epsilon - \epsilon^p) \quad (1), \quad x = \frac{\partial \psi}{\partial c} = ac \quad (2),$$

$$y = \frac{\partial \psi}{\partial p} = v_1(1 - e^{-v_2 p}) + S_y \quad (3), \quad \dot{\epsilon}^p = \lambda \frac{\partial F}{\partial \sigma} = \lambda \frac{(\sigma - x)}{|\sigma - x|} = \lambda S_g \quad (4),$$

$$\dot{p} = -\lambda \frac{\partial F}{\partial y} = \lambda = |\dot{\epsilon}^p| \quad (5) \quad \text{and} \quad \dot{c} = -\lambda \frac{\partial F}{\partial x} = \dot{\epsilon}^p - \frac{b}{a}(x\lambda) \quad (6),$$

where $\lambda \geq 0$, $F \leq 0$, $\lambda F = 0$, are the complementary conditions and λ is the Lagrange multiplier related with the restriction (plasticity criterion) $F \leq 0$.

y is the isotropic hardening, x is the kinematic hardening, p and c are internal variables associated to the isotropic and kinematic hardening respectively, S_y is the elastic limit and a , b , v_1 , v_2 are material parameters.

5. MODELLING THE MATERIAL BEHAVIOUR

From the experimental curves, figure 1, a cyclic softening behaviour of the material has been observed. The material never stabilises and softens continuously until complete failure. Once a crack of significant magnitude was formed, the hysteresis loops were observed to become asymmetric and, in the most of cases, the tests were stopped. In those situations of

continuously softening it is a usual way consider the standard half-life values for a hypothetical stable hysteresis loop.

In the experimental tests, as well, a change is observed in the plastic strain amplitude with the increasing number of cycles. Therefore cyclic softening implicates a change in the anelastic dominion with a consequential change in the accumulated plastic strain, p , cycle by cycle. Considering the continuum elasto-plastic model (where the isotropic hardening, y , related to the accumulated plastic strain, plays an important role during the life of the specimen), the life history is important since the beginning to the end-failure to model the behaviour of themselves. The strong indication of damage effect presence in the specimens observed by a local change of Young modulus (identified by the slope change in the stress-strain loop), is another important consideration. Consequently, in this case, it isn't appropriate estimate a standard stable hysteresis loop at one-half specimen's fatigue life.

Observing the development of the hysteresis loops, the difference between the accumulated plastic strain in a cycle to the consecutive is small: the plastic strain increases slowly. So, the isotropic hardening is very important in the progressive behaviour cycle by cycle but for a single cycle it may be considered constant. Thereby, during a stable loop, the isotropic hardening will be taken constant and only the non-linear kinematic hardening is significant.

Taking into account the above considerations, the choice of the first hysteresis loop are be justified as an hypothetical stable cycle to build the kinematic hardening behaviour. In the elasto-plastic model represented by the set of equations above, the isotropic hardening, equation (3) was constant ($v1 = v2 = 0$) and equal to the elastic limit obtained in the first hysteresis loop:

$$y = S_y \Rightarrow \dot{y} = 0 \quad (3.a)$$

Figure 2 shows the first experimental complete hysteresis loop for the E1 to E6 specimens and figure 3 shows the monotonic, cyclic at middle life and cyclic for the first cycle curves where cyclic softening can be observed.

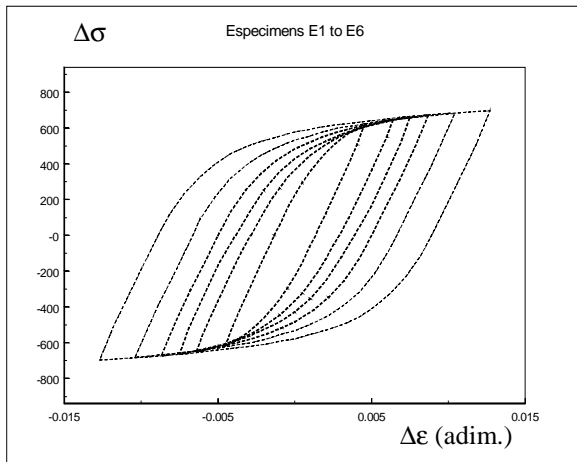


Fig.2 First cycles for the E1 to E6 tests

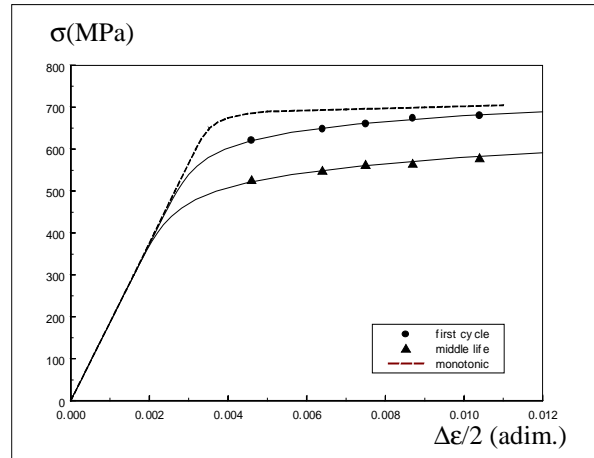


Fig.3 Monotonic vs. cyclic curves

6. PARAMETERS DETERMINATION

Taking into account the above considerations, the kinematic hardening was obtained at the first complete hysteresis loop, for the tests E1 to E6. For the E4 test example, figure 4 shows the experimental stable loop. The experimental curve of stress amplitude versus plastic strain amplitude was obtained directly from the hysteresis loop and the experimental kinematic hardening, x , was extracted by translation of the plastic curve as shown in figure 5.

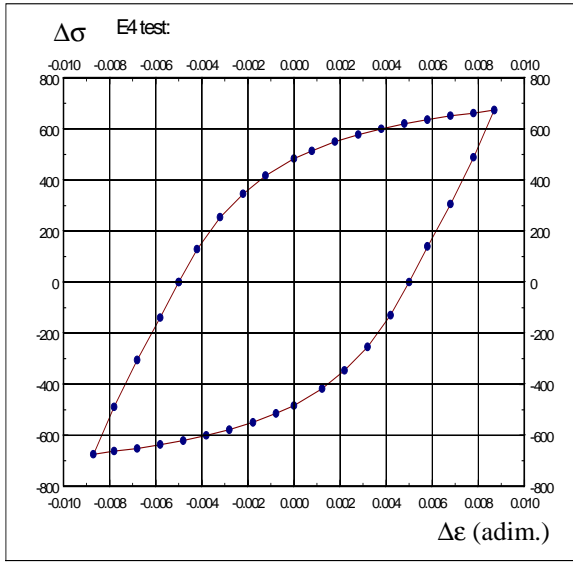


Fig.4 E4: stable hysteresis loop $\Delta\sigma \times \Delta\varepsilon$

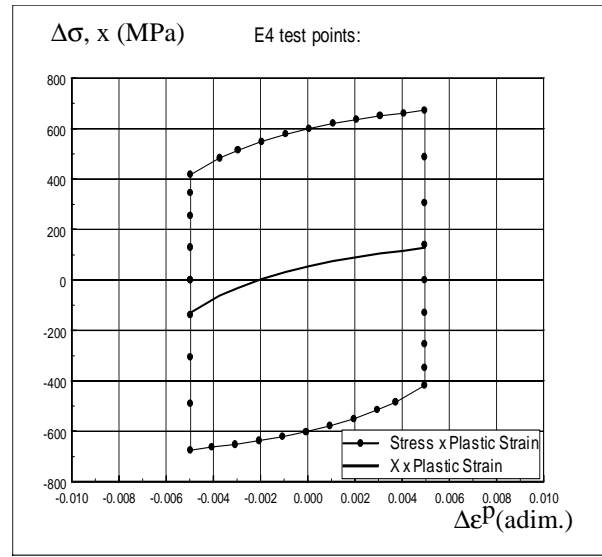


Fig.5 E4: $\Delta\sigma, x \times \Delta\varepsilon^P$

With equation (5), $\dot{p} = \lambda = |\dot{\varepsilon}^P|$, and equation (6), $\dot{c} = \dot{\varepsilon}^P - \frac{b}{a}(x\lambda)$, and replacing in the kinematic evolution law, $\dot{x} = ac$, we obtain,

$$\dot{x} = a\dot{\varepsilon}^P - bx|\dot{\varepsilon}^P| \quad (7)$$

where $\frac{dx}{d\varepsilon^P} = a \mp bx$. Solving the differential equation, we obtain

$$x = -\eta \frac{a}{b} + \left(x_0 + \eta \frac{a}{b} \right) e^{\eta b(\varepsilon^P - \varepsilon_0^P)} \quad (8)$$

in accordance with the non-linear kinematic hardening proposed by Armstrong and Frederick (1966). η represent the sign:

$\eta = -1$ is applied when the direction of the flow is positive (increasing curve), $\lim_{\varepsilon^P \rightarrow \infty} x = a/b$,

the kinematic hardening tends to an asymptotic value, and $\eta = +1$ is applied when the direction of the flow is negative (decreasing curve). ε_0^P and x_0 denote the initial values at known points in the experimental $x \times \varepsilon^P$ curves for each test specimen.

For example, considering the positive direction of flow, $C(\varepsilon_0^P, x_0) = C(0, x_0)$, $\eta = -1$ and adopting $d = a/b$, equation (7) becomes

$$x = d + (x_0 - d)e^{-b\varepsilon^P} \quad (9)$$

Taking 2 points more in each $x \times \varepsilon^P$ curve, a recursive form can be found to obtain the a and b parameters:

$$(x_2 - x_0)e^{-b\varepsilon_1^P} - (x_1 - x_0)e^{-b\varepsilon_2^P} = x_2 - x_1 \quad (10)$$

where $C(0, x_0)$, $P1(\varepsilon_1^P, x_1)$, $P2(\varepsilon_2^P, x_2)$ are points in the experimental curves.

It is interesting to note that the parameters are not constants and tend to asymptotic values when the amplitude of total strain tends to values greater than 2%. Table 3 shown the parameter values related to the test specimens.

Table 3. Experimental values for the kinematic hardening parameters, a and b

Specimen	$\Delta\varepsilon/2$ (%)	$\Delta\varepsilon_p/2$ (%)	$\Delta\sigma/2)_{\max}$ (MPa)	a (GPa)	b
E1	0.46	0.135	622.2	65.63	308
E2	0.64	0.290	647.7	47.05	295
E3	0.75	0.388	660.6	38.00	210
E4	0.87	0.497	674.1	32.70	185
E5	1.04	0.660	680.0	27.89	170
E6	1.27	0.885	696.5	22.92	132

Knowing the experimental values of the parameters a and b above, and using a least-square method, the best representation of themselves can be obtained with sufficiently accurate convergence and determination coefficient. For the parameter a, a good representation was obtained using a third degree polynomial

$$a = 174 - 34950\varepsilon + 2,884,840 \varepsilon^2 - 84,160,460 \varepsilon^3 \quad (11),$$

where ε are adimensional, with determination coefficient $R^2 = 1.0$. A power relation are used for the parameter b

$$b = 4.4729 \varepsilon^{-0.7955} \quad (12)$$

where ε are adimensional, with determination coefficient $R^2 = 0.96$.

It is interesting to observe that when the total strain amplitude tends to values greater than 1.5 % the parameters a and b tend to asymptotic values. It signifies the saturation of the kinematic hardening curve for large strain. Those behaviour are observed in the experimental tests too. Consequently, when the cyclic strain applied exceed 1.5 % ($\Delta\varepsilon/2 > \pm 1.5\%$), the asymptotic values tend to: $a = 15$ GPa and $b = 126$.

Figures 6 and 7 show the experimental points and the curves obtained by the relations (11) and (12). The a and b values are related to total strain for each specimen.

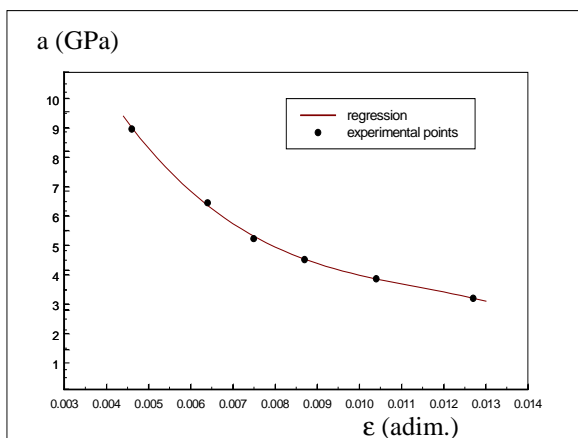


Fig.6 a x ε , regression and experim. points

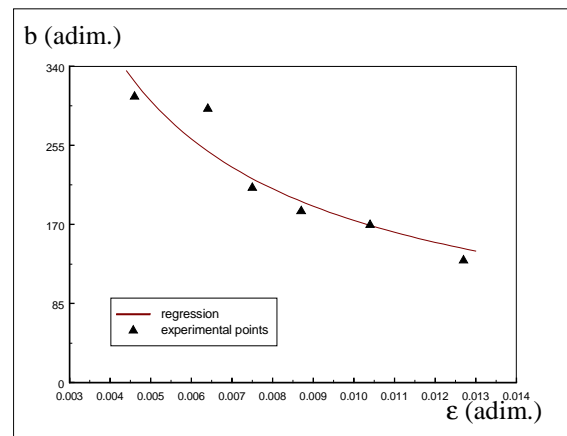


Fig.7 b x ε , regression and experim. points

For the E4 and E5 specimens, figures 8 and 9 compare the non-linear kinematic hardening due to the model and the experimental hardening behaviour, related to plastic strain. This confirms the assumptions made in applying the results to the model.

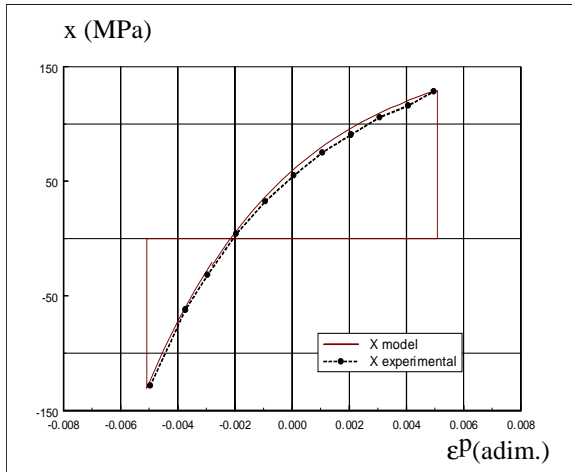


Fig.8 E4: model x test kinematic hardening

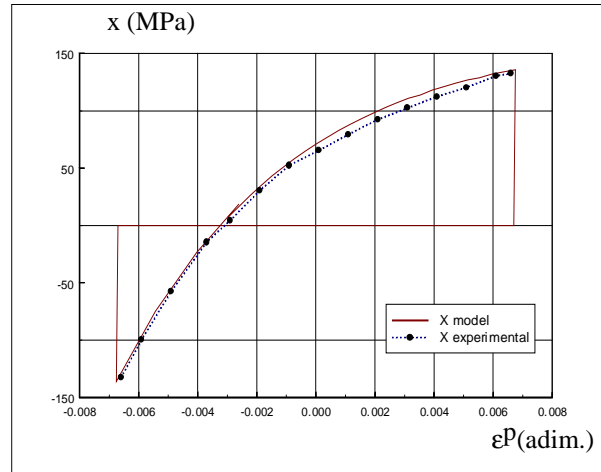


Fig.9 E5: model x test kinematic hardening

7. RESULTS

The model first hysteresis loop and the first experimental hysteresis loop were compared, in terms of stress and total strain. The following figures 10 to 15 show a good agreement of the model results obtained from numerical simulation to the experimental results.

Figure 16 show the closed results between the model cyclic curve and the experimental cyclic curve taken at the first hysteresis loop.

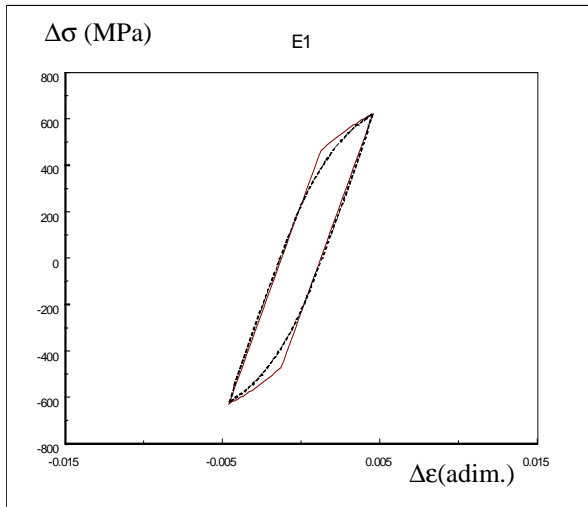


Fig.10 E1: $\Delta\sigma \times \Delta\varepsilon$ $\Delta\varepsilon/2 = 0.35\%$

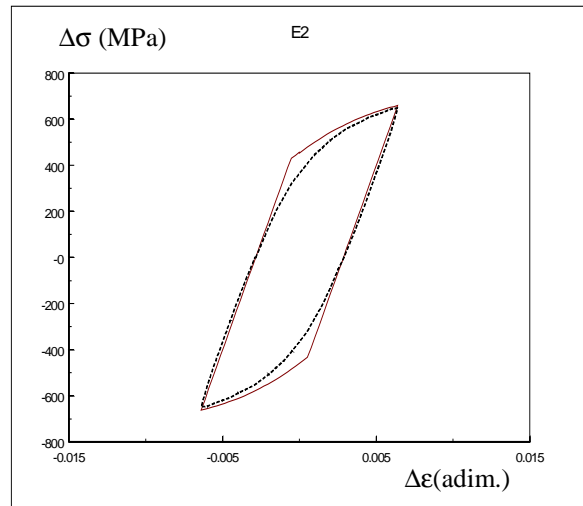


Fig.11 E2: $\Delta\sigma \times \Delta\varepsilon$ $\Delta\varepsilon/2 = 0.64\%$

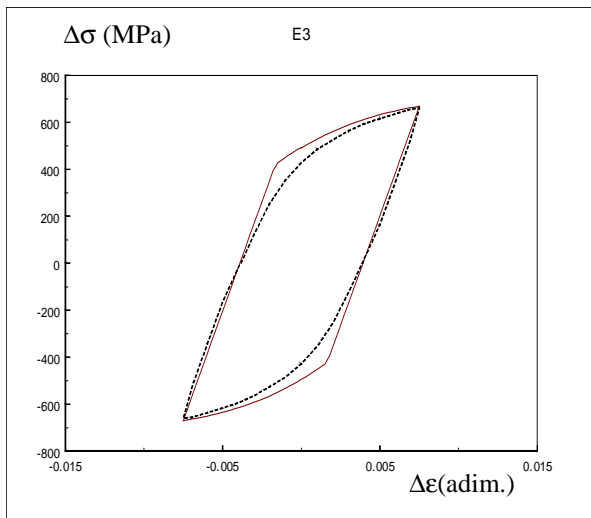


Fig.12 E3: $\Delta\sigma \times \Delta\varepsilon$ $\Delta\varepsilon/2 = 0.75\%$

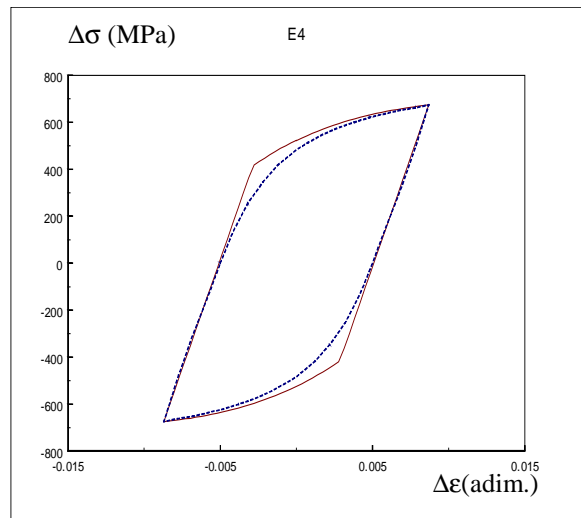


Fig.13 E4: $\Delta\sigma \times \Delta\varepsilon$ $\Delta\varepsilon/2 = 0.87\%$

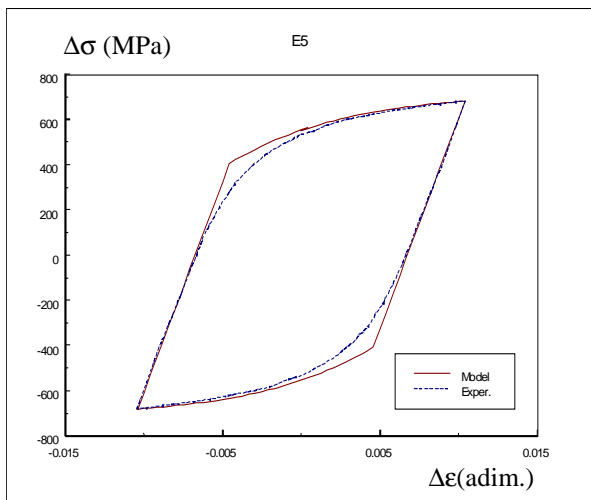


Fig.14 E5: $\Delta\sigma \times \Delta\varepsilon$ $\Delta\varepsilon/2 = 1.04\%$

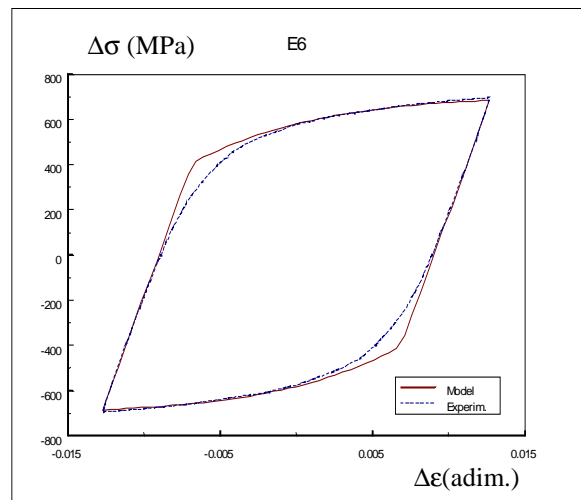


Fig.15 E6: $\Delta\sigma \times \Delta\varepsilon$ $\Delta\varepsilon/2 = 1.27\%$

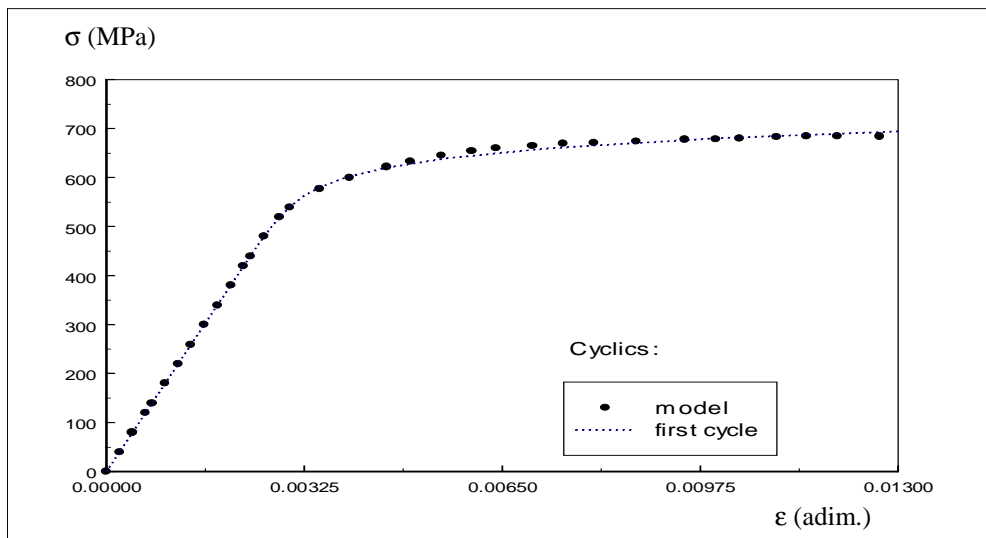


Fig.16 Experimental x model cyclic curves

8. CONCLUDING REMARKS

The ASTM A 471 study becomes interesting due to its continuous softening until fracture occurs. This work is the first step to model the softening behaviour of this steel by a continuum elasto-plastic damage approach. Considering the first cycle as a stable cycle, the isotropic hardening influence must be neglected and a non-linear kinematic hardening law is sufficient to find the model hysteresis loop. The model allows a good results for the elasto-plastic hysteresis loop behaviour and this is fundamental to extend the results into the continuum damage model.

Acknowledgement

Data and tests are obtained in the DIEM-Dipartimento delle Costruzioni Meccaniche, Nucleari e di Metallurgia, Università degli Studi di Bologna, Italia. Our special gratitude to Professor Sergio Curioni the Dean of the Department. The first author is grateful to the CNPq (Brazilian Entity for Scientific and Technological Development) support.

REFERENCES

- Annual Book of ASTM Standards, Standard Specification for Vacuum-Treated Alloy Steel Forgings for Turbine Rotor Disks and Wheels, A 471-94.
- ASTM Standard Practice for Strain-Controlled Fatigue Testing, E 606-92.
- Armstrong, P.J. and Frederick, C. O., A Mathematical Representation of the Multiaxial Bauschinger Effect, C.E.G.B, Report RD/B/N 731, 1966.
- Burden, R.L., Faires, J.D., Reynolds, A.C., Numerical Analysis, Second Edition, PWS Publishers, Boston, Massachusetts, 1981.
- Caligiana, G., Curioni, S., Freddi, A., Fatigue life evaluation in the motor vehicle industries, Int. J. of Vehicle Design, ed. M.A. Dorgham, Inderscience Ltd., U.K., 1987.
- Chaboche, J.L., and Rousselier, G., On the Plastic and Viscoplastic Constitutive Equations – Part I and II, J. of Press. Vessel Technology, Trans. of the ASME, Vol. 105, pp 153-164, May 1983.
- Chimisso, F., Pacheco, P.M.C., Costa Mattos, H., Modelos Continuos Inelásticos: Determinação de Coeficientes Característicos para Materiais Metálicos, Anais COBEM-Congresso Brasileiro de Engenharia Mecânica, Belo-Horizonte, Brasil, 1995.
- Chimisso, F., Pacheco, P.M.C., Costa Mattos, H., Mecânica do Dano Contínuo e Fadiga de Baixo Ciclo: Determinação de Coeficientes Característicos, 9ºSIBRAT/COTEQ, Simpósio Brasileiro sobre Tubulações e Vasos de Pressão, novembro 1996, Rio de Janeiro, Brasil.
- Curioni, S., Freddi, A., Caligiana, G., Life prediction methods for low-cycle torsional fatigue Metals for Structures, Ed. F.M. Mazzolani, RILEM E & FN SPON, pp.162-173, 1992.
- Lemaitre, J. and Chaboche, J.L., Mechanics of Solid Materials, Cambridge University Press, Great Britain, 1994
- Marquis, D., Modelisation et Identification de l' Ecrouissage Anisotrope des Métaux, Thèse de Troisième Cycle, Université de Paris 6, France, 1978.
- Moosbrugger, J. C., and McDowell, D.L., On a Class of Kinematic Hardening Rules for Nonproportional Cyclic Plasticity, J. of Eng. Materials and Technology, Trans. of the ASME, Vol. 111, pp. 87-98, January 1989.
- Wolfram, S., Mathematica, a System for Doing Mathematics by Computer, Second Edition, Addison-Wesley Pub. Co., 1991.